IMA Journal of Applied Mathematics (2011) 1−26
doi: 10.1093/imamat/dri017

Weak interaction of solitary pulses in active dispersive-dissipative nonlinear media

DMITRI TSELUIKO
School of Mathematics, Loughborough University,
Leicestershire, LE11 3TU, UK.

SERAFIM KALLIADASIS
Department of Chemical Engineering, Imperial College London,
London, SW7 2AZ, UK.

We develop an accurate weak-interaction theory for the pulses of the generalised Kuramoto–Sivashinsky (gKS) equation. This equation is the simplest prototype that retains the fundamental mechanisms of wave evolution in nonlinear media, namely, dominant nonlinearity, instability/energy supply, stability/energy dissipation and dispersion. The dynamics of the usual (dispersionless) KS equation is chaotic in both space and time. However, sufficiently strong dispersion regularises the dynamics and the solutions evolve into arrays of interacting pulses, that can form bound states if dispersion does not exceed a certain threshold value. To obtain a theoretical insight into the interaction of the pulses, we represent a solution of the gKS equation as a superposition of pulses and an overlap function, and we carefully derive a coupled system of ordinary differential equations describing the evolution of the locations of the pulses by projecting the dynamics onto translational modes. This approach allows to analyse bound states of the pulses and to derive a criterion on the existence of a countable infinite or finite number of bound states, depending on the strength of the dispersive term in the equation, which is in agreement with Shilnikov's criterion on the existence of subsidiary homoclinic orbits. We consider in detail two- and three-pulse bound states. We compare the interaction theory with computations of the full equation when the initial condition is a superposition of two or three pulses, and in all cases we find very good agreement.

Keywords: solitary pulse interaction, generalised Kuramoto-Sivashinsky equation.

1. Introduction

In this study, we analyse the interaction dynamics of the solitary-pulse solutions of the generalised Kuramoto-Sivashinsky (gKS) equation,

$$h_t + hh_\xi + h_{\xi\xi} + \delta h_{\xi\xi\xi} + h_{\xi\xi\xi\xi} = 0, \quad t \in [0,\infty), \quad \xi \in (-\infty,\infty). \tag{1.1}$$

This equation represents the simplest possible prototype that retains the fundamental elements of any active nonlinear medium that involves wave evolution, namely, the dominant nonlinearity hh_ξ, the destabilising term $h_{\xi\xi}$, the stabilising term $h_{\xi\xi\xi\xi}$, and the dispersive term $\delta h_{\xi\xi\xi}$, where δ a parameter that measures the relative importance of dispersion compared to the other effects. For systems whose spatial average does not drift, the functional form of the quadratic nonlinearity can be easily obtained from symmetry considerations, as the only other dominant quadratic nonlinearity, h^2, is obviously ruled out.

The gKS equation has been derived in numerous physical contexts, from plasma waves with dispersion due to finite ion banana width (Cohen *et al.*, 1976) to fluid dynamics, i.e. liquid films in various settings and small-amplitude disturbances as well as near-critical conditions: Films flowing down along

© Institute of Mathematics and its Applications 2005; all rights reserved.

a flat substrate (Kalliadasis *et al.*, 2012), films sheared by a turbulent gas (Jurman & McCready, 1989), falling liquid films in the presence of a viscous stress at the free surface (Oron & Edwards, 1993), liquid films flowing down a uniformly heated wall (Kalliadasis *et al.*, 2003) and reactive falling films (Trevelyan & Kalliadasis, 2004). Recently, the gKS equation was also reported for liquid films coating vertical fibres and was successfully used to explain experimental observations on interactions of drop-like pulses on such films (Duprat *et al.*, 2009; Tseluiko *et al.*, 2010).

In the context of liquid films, h, ξ and t denote appropriately scales film amplitude, streamwise coordinate and time. The terms hh_x, h_{xx}, h_{xxx} and h_{xxxx}, are often due to the interfacial kinematics associated with mean flow, inertia, viscosity and surface tension, respectively, and δ is a combination of dimensionless parameters expressing the relative importance of inertia, viscosity and surface tension, i.e. Reynolds and Weber numbers (Kalliadasis *et al.*, 2012). The limit $\delta \to \infty$ leads to a perturbed Korteweg-de Vries (KdV) equation (Kawahara, 1983; Kawahara & Toh, 1988) (but strictly speaking the degeneracy of the KdV one-parameter infinite family of solutions is broken by the instability and stability terms, Saprykin, 2005), while in the limit $\delta \to 0$ the usual KS equation is recovered. This equation was first derived by Homsy (1974), Lin (1974), and Nepomnyashchy (1974) in the context of falling liquid films (for small amplitude disturbances but sufficiently far from criticality (Kalliadasis *et al.*, 2012) and also in chemical physics to describe propagation of concentration waves by Kuramoto (1978), flame-front instabilities and combustion dynamics by Sivashinsky (1977), and many other physical contexts.

The KS equation has been extensively studied both analytically and numerically, and it has been established that it leads to complicated chaotic dynamics in both space and time if the domain size is sufficiently large (e.g. Hyman *et al.*, 1986). However, as was first shown by Kawahara (1983), sufficiently strong dispersion (i.e. δ is sufficiently large) arrests the spatio–temporal chaos and the solution evolves into a row of well-defined interacting coherent structures of approximately the same shape, each of which resembling the infinite-domain one-hump solitary pulse. [Hence, the gKS equation can also serve as a paradigmatic model for the study of (low-dimensional) spatio-temporal chaos or "weak/dissipative turbulence as defined by Manneville Manneville (1990).] These coherent structures slowly attract or repel each other and their dynamic interaction with continuously varying separation seems to persist indefinitely. Our aim here is to develop a weak-interaction theory of such pulses and to derive a system of ordinary differential equations describing accurately the dynamics of the locations of the pulses. Weak-interaction theories have been constructed for many physical systems (see, for example, Ei, 2002; Sandstede, 2002). Most weak-interaction theories are approximate and derived using physical arguments. Rigorous justification of such theories is highly non-trivial and has been achieved for some cases, where the primary pulse is spectrally stable (Ei, 2002; Zelik & Mielke, 2009). As far as the gKS equation is concerned, previous efforts to develop weak-interaction approaches, include those by Elphick *et al.* (1991), Ei & Ohta (1994), Chang & Demekhin (2002). However, in these studies certain crucial technical details have been overlooked and as a result the corresponding weak-interaction theories are not accurately constructed. For instance, the spectra of the operator of the equation linearised around a pulse and its adjoint have not been analysed carefully. This is a crucial step for developing a pulse interaction theory based on appropriate projections onto the corresponding null spaces. Other particular details that were overlooked by previous authors will be discussed later on.

In section 2. we outline our weak-interaction theory for pulses of the gKS equation. In section 3. we analyse formation of bound states of pulses. In section 4. we compare theoretical predictions with numerical experiments. In section 5. we close with conclusions.

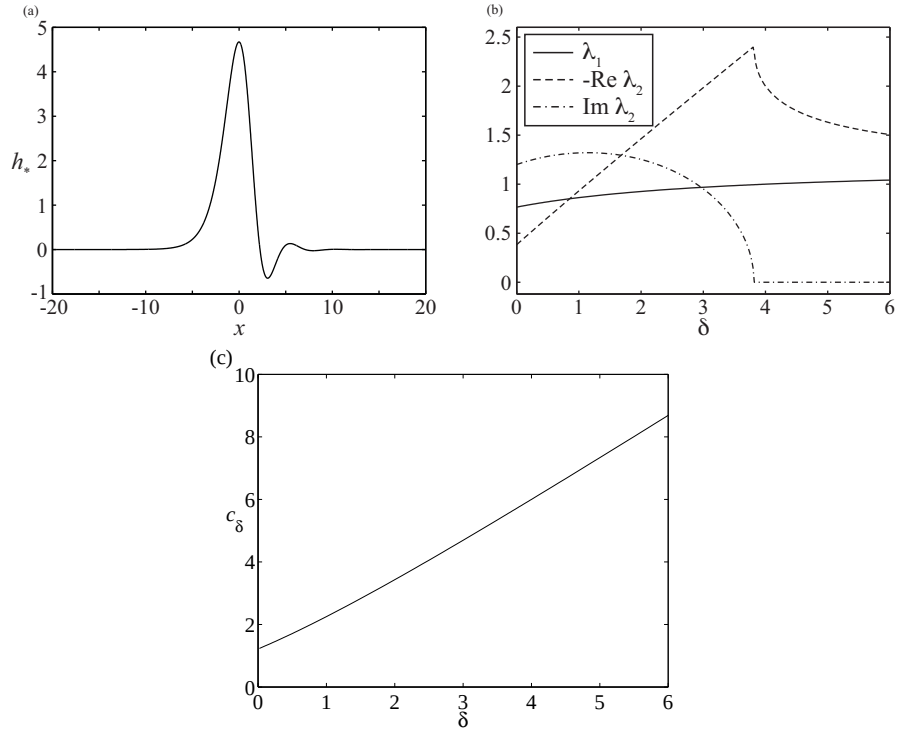

FIG. 1. (a) A stationary solitary pulse of the gKS equation for $\delta = 0.5$. The speed of the pulse is $c_\delta \approx 1.71$. (b) Dependence of root λ_1 and the real and imaginary parts of root λ_2 (solid, dashed and dot-dashed lines, respectively) of (2.6) on δ. **(c) Dependence of the pulse velocity c_δ on δ.**

2. Pulse-interaction theory for the gKS equation

In a frame moving with the velocity c_δ of a pulse, the gKS equation (1.1) becomes

$$h_t - c_\delta h_x + hh_x + h_{xx} + \delta h_{xxx} + h_{xxxx} = 0, \tag{2.1}$$

where $x = \xi - ct$. Let $h_* = h_*(x)$ be a stationary pulse. It satisfies the steady version of equation (2.1),

$$-c_\delta h_{*x} + h_* h_{*x} + h_{*xx} + \delta h_{*xxx} + h_{*xxxx} = 0, \tag{2.2}$$

and tends to zero at infinity. We additionally require that h_* attains its maximum value at $x = 0$. We consider one-hump pulses only, since they are the main feature of the evolution of the solutions of the gKS equation following destabilisation of the trivial solution $h \equiv 0$ (e.g. Kawahara, 1983; Kawahara & Toh, 1988). Integrating (2.2) and applying the conditions at infinity gives

$$-c_\delta h_* + \frac{1}{2}h_*^2 + h_{*x} + \delta h_{*xx} + h_{*xxx} = 0, \tag{2.3}$$

a nonlinear eigenvalue problem for the pulse speed c_δ. This is solved numerically with a pseudospectral scheme in a periodic domain in which we take the Fast Fourier Transform (FFT) of (2.3) to obtain

a system of nonlinear equations for the unknown FFT of the pulse and the pulse speed. The system was solved using Newton's iteration by choosing an appropriate initial guess. A detailed review of computational methodologies for localised nonlinear structures is given by Champneys & Sandstede (2007). An example of a stationary pulse is shown in Fig. 1(a) for $\delta = 0.5$.

The tails of $h_*(x)$ behave as follows (see Kawahara & Toh, 1988):

$$h_0(x) \sim C_1 \mathrm{e}^{\lambda_1 x} \qquad \text{as } x \to -\infty, \tag{2.4}$$

$$h_0(x) \sim \mathrm{Re}(C_2 \mathrm{e}^{\lambda_2 x}) \quad \text{as } x \to \infty, \tag{2.5}$$

where C_1 is a real constant and C_2 is, in general, a complex one, λ_1 and λ_2 are non-zero roots of the characteristic equation of the linearised stationary equation (2.3):

$$\lambda^3 + \delta\lambda^2 + \lambda - c_\delta = 0. \tag{2.6}$$

One root, which is denoted by λ_1 is always real and positive, so that the left tail is monotonic. If δ is below the threshold value $\delta^* \approx 3.71$, there is a pair of complex conjugate roots, λ_2 and $\bar{\lambda}_2$, with negative real parts, so that the right tail is oscillatory. Otherwise, if δ is above δ^*, there are two real roots with negative real parts, so that the right tail is monotonic as well. In this case, λ_2 denotes the root with larger real part. The dependencies of the root λ_1 and the real and imaginary parts of the root λ_2 on δ are shown in Fig. 1(b). **Fig. 1(c) shows the dependence of the pulse velocity, c_δ, on δ (note that for large δ, $c_\delta \sim 1.4\delta$, see Chang & Demekhin, 2002).** We note that the solitary pulse can be considered as a homoclinic orbit in a three-dimensional phase space connecting the origin with itself and given parametrically by $x \mapsto \big(h_*(x), h_*'(x), h_*''(x)\big)$ for $x \in (-\infty, \infty)$. The origin is a saddle-focus if $\delta < \delta^*$ and a saddle if $\delta > \delta^*$.

From now on, we consider the gKS equation in the frame moving with the velocity c_δ of a stationary pulse, i.e. equation (2.1). As noted in the introduction, computational experiments show that for sufficiently large δ the dynamics is dominated by one-hump pulses that slowly repel and attract each other. Therefore, we assume that the solution, h, is described as a superposition of quasi-stationary pulses h_i, $i \in S$, (where either $S = \{1, 2, \ldots, n\}$, or $S = \mathbb{Z}^+$, or $S = \mathbb{Z}^-$, or $S = \mathbb{Z}$) located at $x_i(t)$, namely,

$$h_i(x,t) = h_*(x - x_i(t)), \qquad i \in S, \tag{2.7}$$

and a small overlap (or correction) function, $\hat{h} = \hat{h}(x,t)$, which is assumed to be "free of translational modes" since possible changes of the locations of the pulses are already taken into account by the fact that we allow the x_i's to depend on time. The exact meaning of the phrase "free of translational modes" will be specified later on. Thus, we use the following ansatz for the solution:

$$h = \sum_{i \in S} h_i + \hat{h}, \tag{2.8}$$

and aim to derive a system of equations governing the locations of the pulses. A schematic representation is shown in Fig. 2. We assume that $x_i < x_j$ for $i < j$, and we denote the separation distances by l_i's, namely, $l_i = x_{i+1} - x_i$. We assume that $l^* = \inf l_i \gg 1$ and introduce a small parameter $\varepsilon = \exp(-\min\{\lambda_1, -\mathrm{Re}\,\lambda_2\} l^*)$. Substituting (2.8) into (2.1) gives

$$\hat{h}_t - \sum_{i \in S} x_i'(t) h_{ix} - c_\delta \hat{h}_x + \hat{h}_{xx} + \delta \hat{h}_{xxx} + \hat{h}_{xxxx} + \sum_{\substack{i,j \in S \\ i \neq j}} h_i h_{jx} + \sum_{i \in S} (h_i \hat{h})_x + \hat{h}\hat{h}_x = 0. \tag{2.9}$$

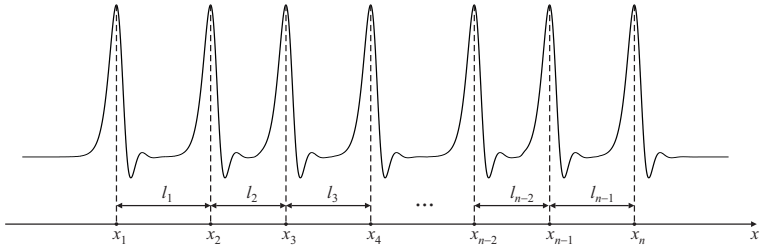

FIG. 2. Schematic representation of a superposition of n pulses located at $x_1, \ldots, x_n$.

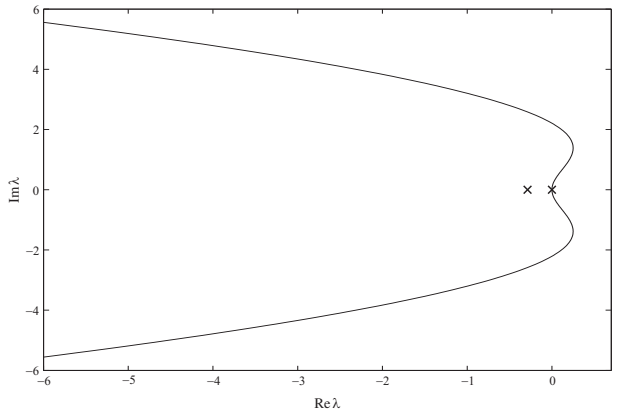

FIG. 3. Spectrum of $\mathscr{L}_k$ for $\delta = 0.5$. The solid line indicates the essential part, whilst the crosses indicate the point spectrum.

For each $k \in S$, we rewrite this equation as follows:

$$\begin{aligned} \hat{h}_t - x_k'(t)h_{kx} - \mathscr{L}_k\hat{h} = \quad & - \quad (h_{k-1}h_k)_x - (h_k h_{k+1})_x \\ & - \sum_{\substack{i,j\in S, i<j \\ i\neq k,\, j\neq k}} (h_i h_j)_x - \sum_{\substack{i\in S \\ i\neq k}} (h_i\hat{h})_x - \hat{h}\hat{h}_x + \sum_{\substack{i\in S \\ i\neq k}} x_i'(t)h_{ix}, \end{aligned} \tag{2.10}$$

where h_{k-1} or h_{k+1} is replaced with zero if $k-1 \notin S$ or $k+1 \notin S$, respectively. $\mathscr{L}_k$ is a linear operator defined by

$$\mathscr{L}_k f = c_\delta f_x - f_{xx} - \delta f_{xxx} - f_{xxxx} - (h_k f)_x. \tag{2.11}$$

The formal adjoint operator, $\mathscr{L}_k^*$, with respect to the usual inner product in $L^2_{\mathbb{C}}$ is given by

$$\mathscr{L}_k^* f = -c_\delta f_x - f_{xx} + \delta f_{xxx} - f_{xxxx} + h_k f_x. \tag{2.12}$$

Our next objective is to analyse the spectra of the operators $\mathscr{L}_k$ and $\mathscr{L}_k^*$. A description of methods used to analyze spectra of non-self-adjoint differential operators is given, for example, by Davies (2002). Since $\mathscr{L}_k$ is a relatively compact perturbation of the operator $-c_\delta\partial_x - \partial_x^2 + \delta\partial_x^3 - \partial_x^4$, the essential spectra of these operators coincide (e.g. Edmunds & Evans, 1987; Pego & Weinstein, 1992). Thus, by

applying the Fourier transform for the latter operator, we find that the essential spectrum of $\mathscr{L}_k$ is the following set in the complex plane:

$$\{\mathrm{i}c_\delta\kappa+\kappa^2+\mathrm{i}\delta\kappa^3-\kappa^4:\ \kappa\in\mathbb{R}\}, \tag{2.13}$$

shown as a solid line in Fig. 3. Similarly, we find that the essential spectrum of $\mathscr{L}_k^*$ is given by the same set in the complex plane.

We now note the following properties of $\mathscr{L}_k$ and $\mathscr{L}_k^*$ (see Frisch *et al.*, 1986):

$$\mathscr{L}_k h_{kx}=0, \qquad \mathscr{L}_k(-1)=h_{kx}, \qquad \mathscr{L}_k^* 1=0. \tag{2.14}$$

From (2.14) it follows that, when considered on a periodic interval, h_{kx} and 1 are a zero eigenfunction and a zero adjoint eigenfunction for $\mathscr{L}_k$, respectively. Besides, -1 is a generalised zero eigenfunction. We conclude that on a periodic interval, zero is an eigenvalue of algebraic multiplicity at least two and geometric multiplicity at least one.

The zero eigenfunction $\Phi_1^k=h_{kx}$ is associated with the translational symmetry of the gKS equation, and we refer to this eigenfunction as the translational mode. The existence of a zero eigenfunction associated with the translational symmetry of the gKS equation is known from previous studies on the equation (e.g. Chang & Demekhin, 2002). In fact, this is true for any equation with translational symmetry:

Proposition 1. Let us assume that the equation

$$h_t=\mathscr{K}_\delta[h]+\mathscr{N}[h], \tag{2.15}$$

has the translational symmetry, where $\mathscr{K}_\delta$ is a linear differential operator that is a polynomial in ∂_x and $\mathscr{N}$ is a nonlinear operator that is defined through a pointwise evaluation of h and its derivatives. Then, h_{*x} is a zero eigenfunction of the following operator:

$$\mathscr{L}[f]\equiv c_\delta f_x+\mathscr{K}_\delta[f]+\mathscr{D}_{h_*}\mathscr{N}[f]. \tag{2.16}$$

where $h_*(x)$ is a stationary solution of

$$h_t=ch_x+\mathscr{K}_\delta[h]+\mathscr{N}[h] \tag{2.17}$$

for some $c=c_\delta$, and $\mathscr{D}_{h_*}\mathscr{N}$ is the linearization of $\mathscr{N}$ at h_*, i.e. such an operator that

$$\mathscr{N}[h_*+\varepsilon f]=\mathscr{N}[h_*]+\varepsilon\,\mathscr{D}_{h_*}\mathscr{N}[f]+O(\varepsilon^2). \tag{2.18}$$

(Rigorously, $\mathscr{D}_{h_*}\mathscr{N}$ can be defined as the Fréchet derivative of the nonlinear operator $\mathscr{N}$ at h_*. For the gKS equation, $\mathscr{D}_{h_*}\mathscr{N}[f]\equiv-(h_*f)_x$.)

As far as the generalised adjoint eigenfunction, $\Phi_2^k=-1$, is concerned, it is associated with another more subtle invariance, the Galilean symmetry. If h_* is a solution of the stationary gKS equation written in the frame moving with velocity c_δ, then $h_*+\sigma$ is a solution of the stationary gKS equation written in the frame moving with velocity $c_\delta+\sigma$. The existence of this eigenfunction for the gKS equation is also known from previous studies on the equation, e.g. Elphick *et al.* (1991), while for the KS equation its existence was shown by Frisch *et al.* (1986). As a matter of fact, it can be easily shown that the following more general statement holds:

Proposition 2. Let us assume in addition to Proposition 1 that for each c there is a stationary solution of (2.17), $h(c,x)$, such that the dependence on c is smooth and $h(c_\delta,x)=h_*(x)$. Then $-\partial h/\partial c|_{c=c_\delta}$ is a generalised zero eigenfunction of the operator $\mathscr{L}$ defined by (2.16).

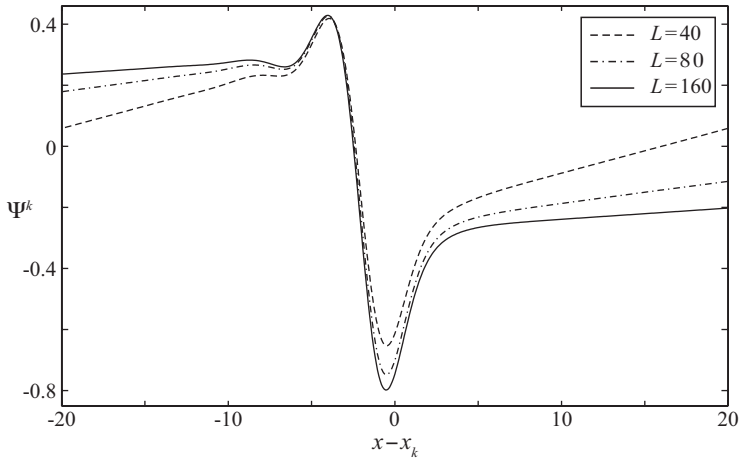

FIG. 4. Numerically computed generalised adjoint eigenfunctions Ψ_2^k for $\delta = 0.5$ on the interval $[-L, L]$ for $L = 40$, 80 and 160 (dashed, dot-dashed and solid lines, respectively).

For the gKS equation, $h(c, x) = h_*(x) + c - c_\delta$, i.e. $\partial h/\partial c = 1$. For these reasons, we refer to the generalised adjoint eigenfunction, $\Phi_2^k = -1$, as the Galilean or speed mode.

To analyse numerically the spectrum of $\mathscr{L}_k$, we consider this operator on a finite interval, $[-L, L]$, and impose periodic boundary conditions: As was shown by Sandstede & Scheel (2000) that periodic boundary conditions reproduce accurately the point and the essential spectra of the operators on unbounded domains, if the period is sufficiently large. Our results reveal that, in addition to the essential spectrum and the zero eigenvalue that is embedded into the essential spectrum, there is one more eigenvalue that is negative and isolated (the eigenvalues are shown as crosses in Fig. 3). Moreover, our numerical results confirmed that zero is an eigenvalue of algebraic multiplicity exactly two and geometric multiplicity exactly one.

As is evident from (2.14), the eigenfunction of $\mathscr{L}_k^*$ on a periodic domain corresponding to the zero eigenvalue is a constant. We normalise it so that its inner product with $\Phi_2^k = -1$ is unity, i.e. we choose $\Psi_1^k = -1/2L$. Numerically, however, we obtain that zero is an eigenvalue of $\mathscr{L}_k^*$ of algebraic and geometric multiplicities two and unity, respectively, as expected. Unlike the generalised eigenfunction Φ_2^k, we do not have an analytic expression for the adjoint generalised eigenfunction Ψ_2^k and it must be obtained numerically. The results are shown in Fig. 4 for various values of the period. The normalizations are chosen so that the following conditions hold:

$$\langle \Phi_1^k, \Psi_1^k \rangle = 0, \qquad \langle \Phi_1^k, \Psi_2^k \rangle = 1, \tag{2.19}$$

$$\langle \Phi_2^k, \Psi_1^k \rangle = 1, \qquad \langle \Phi_2^k, \Psi_2^k \rangle = 0. \tag{2.20}$$

Here, $\langle \cdot, \cdot \rangle$ denotes the usual inner product in $L^2_{\mathbb{C}}(-L, L)$.

Let us now discuss what happens in the limit $L \to \infty$. First, $\|\Phi_2^k\| \to \infty$, i.e. we must exclude Φ_2^k from our consideration, meaning that zero becomes an eigenvalue of both algebraic and geometric multiplicity unity for the operator $\mathscr{L}_k$. Also, $\Psi_1^k \to 0$ (pointwise). Therefore, $\mathscr{L}_k^* \Psi_2^k \to 0$ (pointwise), meaning that Ψ_2^k tends pointwise to a function that is in the null space of $\mathscr{L}_k^*$. As our numerical results show, Ψ_2^k tends to a function that has a jump at infinity as $L \to \infty$. We denote this function by Ψ^k. The existence

of a function with a jump at infinity that belongs to the null space of $\mathscr{L}_k^*$ on an infinite interval has also been noticed by Elphick *et al.* (1991). We also conclude that the existence of a localised function in the null space of $\mathscr{L}_k^*$ tending to zero at infinity stated by Chang & Demekhin (2002) is erroneous; such a function does not exist. It can be easily verified that for the KdV equation (which is recovered in the limit $\delta \to \infty$) the solitary pulse itself is a zero eigenfunction of the adjoint operator (see Ei & Ohta, 1994). Ei & Ohta (1994) used this to postulate that there is a zero adjoint eigenfunction for the general case, when $\varepsilon \neq 0$, which for small ε could be found in terms of a perturbation expansion in ε. However, this is not the case, since any non-zero ε implies that the non-constant function from the null space of $\mathscr{L}_k^*$ has a jump at infinity meaning that it is not in $L^2_{\mathbb{C}}$.

To conclude, on an infinite domain zero is an eigenvalue of $\mathscr{L}_k$ of both algebraic and geometric multiplicities unity. The null space is spanned by $\Phi^k = \lim_{L\to\infty} \Phi_1^k$. For $\mathscr{L}_k^*$, there are no bounded eigenfunctions in $L^2_{\mathbb{C}}$, i.e. strictly speaking zero is not in the point spectrum of $\mathscr{L}_k^*$ on an infinite interval. The null space of $\mathscr{L}_k^*$ is spanned by a constant and a function having a jump at infinity, Ψ^k. **Note that the existence of the function Ψ^k that belongs to the null space of $\mathscr{L}_k^*$ and tends to different constants at $-\infty$ and $+\infty$ can be understood analytically. Indeed, let us consider the operator $\widetilde{\mathscr{L}_k}$ given by**

$$\widetilde{\mathscr{L}_k} f = c_\delta f_x - \delta f_{xx} - f_{xxx} - h_k f. \tag{2.21}$$

(Note that $\mathscr{L}_k = \partial_x \circ \widetilde{\mathscr{L}_k}$). The operator $\widetilde{\mathscr{L}_k}$ is Fredholm (e.g. Edmunds & Evans (1987)) with one-dimensional null space spanned by h_{kx}. Therefore, there exists the adjoint null eigenfunction, which we denote by ψ^k. Then, since $\mathscr{L}_k^* = -\widetilde{\mathscr{L}_k^*} \circ \partial_x$, we observe that any constant belongs to the null space of $\mathscr{L}_k^*$ and the integral of ψ^k, which we denote by Ψ^k (i.e. $\psi^k = \Psi^k_x$) belongs to the null space of $\mathscr{L}_k^*$. Since there is no reason for the integral of ψ^k over the whole real line to vanish (and it indeed does not vanish as our results show), the function Ψ^k tends to different constants at $-\infty$ and $+\infty$ and, therefore, does not belong to L^2.

We aim to project the dynamics onto translational modes, i.e. the null spaces of $\mathscr{L}_k$. The fact that zero is not an isolated eigenvalue of $\mathscr{L}_k$ and also not in the point spectrum of $\mathscr{L}_k^*$ complicates rigorous projections onto the translational modes, but we may still define formally the following projection operators:

$$\Pi_k(f) = \int_{-\infty}^{\infty} f \Psi^k \, \mathrm{d}x. \tag{2.22}$$

At this stage, we give a precise meaning to the phrase "$\hat{h}$ is free of translational modes". Strictly speaking, it means that for each $k \in S$, $\Pi_k(\hat{h}) = 0$. Equivalently, this means that x_k, $k \in S$, are defined so that

$$\int_{-\infty}^{\infty} \Big(h(x,t) - \sum_{i=1}^{n} h_*(x - x_i(t)) \Big) \Psi(x - x_k(t)) \, \mathrm{d}x = 0 \tag{2.23}$$

for each $k \in S$, where Ψ is such that $\Psi^k(x,t) = \Psi(x - x_k(t))$. Next, we apply projections Π_k to (2.10), which leads to

$$\begin{aligned} x_k' = {} & \Pi_k((h_{k-1}h_k)_x) + \Pi_k((h_k h_{k+1})_x) + \sum_{\substack{i,j\in S,\, i<j \\ i\neq k,\, j\neq k}} \Pi_k((h_i h_j)_x) \\ & + \sum_{\substack{i\in S \\ i\neq k}} \Pi_k((h_i\hat{h})_x) + \Pi_k(\hat{h}\hat{h}_x) - \sum_{\substack{i\in S \\ i\neq k}} x_i' \Pi_k(h_{ix}) - x_k' \Pi_k(\hat{h}_x), \end{aligned} \tag{2.24}$$

where the first or the second term on the right-hand side should be neglected if $k-1 \notin S$ or $k+1 \notin S$, respectively. The latter expression is exact, but we wish to neglect some terms in it. This is done by additionally assuming that $\hat{h}$ is $O(\varepsilon)$ and by noting that

$$\Psi(x) \sim \mathrm{Re}(A_1 \mathrm{e}^{\lambda_2 x}) + d \quad \text{as } x \to -\infty, \tag{2.25}$$

$$\Psi(x) \sim A_2 \mathrm{e}^{\lambda_1 x} - d \quad \text{as } x \to \infty, \tag{2.26}$$

where A_1 is a complex constant and A_2 and d are real constants. Then it follows that x_k' is $O(\varepsilon)$ and also

$$\sum_{\substack{i,j\in S, i<j \\ i\neq k,\, j\neq k}} \Pi_k((h_i h_j)_x), \sum_{\substack{i\in S \\ i\neq k}} \Pi_k((h_i \hat{h})_x), \Pi_k(\hat{h}\hat{h}_x), \sum_{\substack{i\in S \\ i\neq k}} x_i'(t)\Pi_k(h_{ix}), x_k'\Pi_k(\hat{h}_x) \tag{2.27}$$

are all $O(\varepsilon^2)$. Keeping $O(\varepsilon)$ terms in (2.24) and neglecting $O(\varepsilon^2)$ terms, we find

$$x_k' = S_2(x_k - x_{k-1}) + S_1(x_{k+1} - x_k), \quad k \in S, \tag{2.28}$$

where S_1 and S_2 are defined as follows:

$$S_{1,2}(l) \equiv -\int_{-\infty}^{\infty} h_*(x+l/2)h_*(x-l/2)\Psi_x(x \pm l/2)\,\mathrm{d}x. \tag{2.29}$$

In (2.28) the first or the second term on the right-hand side should be neglected if $k-1 \notin S$ or $k+1 \notin S$, respectively. On a periodic interval $[-L, L]$ we obtain the following system for n pulses:

$$x_1' = S_2(x_1 - x_n + 2L) + S_1(x_2 - x_1), \tag{2.30}$$

$$x_k' = S_2(x_k - x_{k-1}) + S_1(x_{k+1} - x_k), \ 1 < k < n, \tag{2.31}$$

$$x_n' = S_2(x_n - x_{n-1}) + S_1(x_1 - x_n + 2L). \tag{2.32}$$

It is noteworthy that projections onto translational modes can be made rigorous by choosing an appropriate weighted space, namely, $L^2_a = \{f : \mathrm{e}^{ax} f \in L^2_{\mathbb{C}}\}$, where $a > 0$, with the inner product $\langle f, g\rangle_a = \langle \mathrm{e}^{ax} f, \mathrm{e}^{ax} g\rangle$, where $\langle \cdot, \cdot \rangle$ denotes the usual inner product in $L^2_{\mathbb{C}}$. The use of the weighted space for the KdV equation was justified by Pego & Weinstein (1994). As noticed by these authors, studying the spectrum of $\mathscr{L}_k$ in L^2_a is equivalent to studying the spectrum of the operator defined by $\mathscr{L}_k^a f = \mathrm{e}^{ax}\mathscr{L}_k(\mathrm{e}^{-ax} f)$ on $L^2_{\mathbb{C}}$. We can easily obtain that the essential spectrum of $\mathscr{L}_k^a$ is given by

$$\{\mathrm{i}c_\delta(\kappa + \mathrm{i}a) + (\kappa + \mathrm{i}a)^2 + \mathrm{i}\delta(\kappa + \mathrm{i}a)^3 - (\kappa + \mathrm{i}a)^4 : \kappa \in \mathrm{R}\}. \tag{2.33}$$

For sufficiently small a, the essential spectrum of $\mathscr{L}_k^a$ is shifted to the left in the complex plane compared to the essential spectrum of $\mathscr{L}_k$. This can be seen in Fig. 5(a), where the essential spectrum of $\mathscr{L}_k^a$ is plotted for $a = 0, 0.1, 0.2$, and 0.3. It is also interesting to note that for certain values of a, the essential spectrum can be completely moved to the left half of the complex plane, i.e. the pulses become spectrally stable in the weighted space. For example, we find that for $\delta = 0.5$, the essential spectrum of $\mathscr{L}_k^a$ belongs to the left half-plane for $a_1 < a < a_2$, where $a_1 \approx 0.11$ and $a_2 \approx 0.64$. This means that for the values of δ for which it is possible to shift the essential spectrum to the left half-plane and also $a_1 < -\mathrm{Re}\,\lambda_2$, the pulses of the gKS equation tolerate any sufficiently small perturbations that decay to zero sufficiently fast as $x \to \infty$ (i.e. a perturbation must be $o(\mathrm{e}^{-a_1 x})$ as $x \to \infty$), see Sandstede (2002)

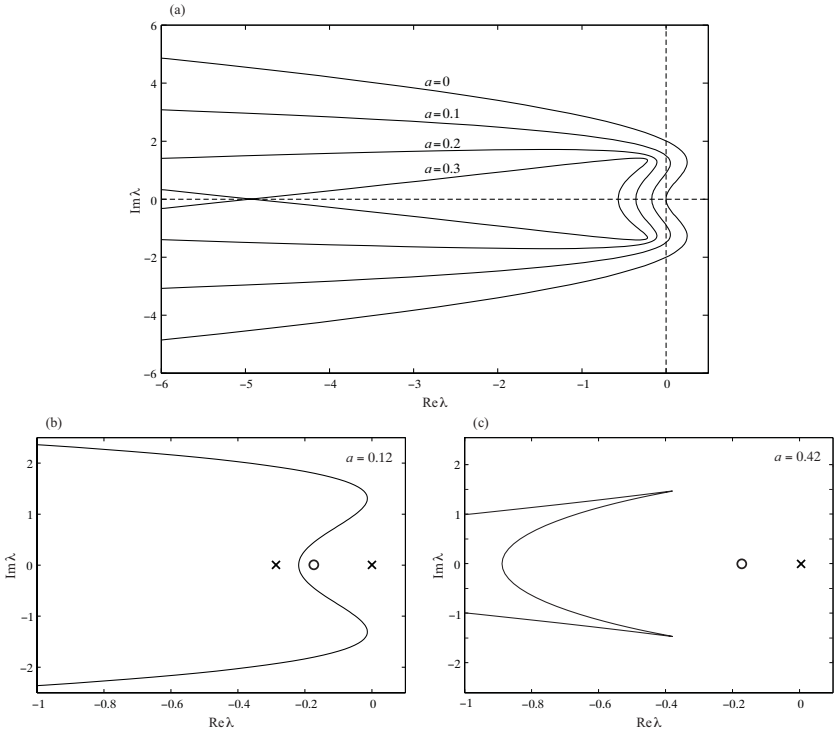

FIG. 5. (a) Essential spectrum of $\mathscr{L}_k^a$ for $a = 0$, 0.1, 0.2 and 0.3 when $\delta = 0.5$. (b) and (c) show spectra of $\mathscr{L}_k^a$ for $a = 0.12$ and $a = 0.42$, respectively, when $\delta = 0.5$. The solid lines indicate the essential part, the crosses indicate the eigenvalues that are also the eigenvalues of $\mathscr{L}_k$ (for $a = 0.42$ one of the eigenvalues disappears), the circles indicate the resonance pole, i.e. the eigenvalue of $\mathscr{L}_k^a$ that is not the eigenvalue of $\mathscr{L}_k$ (this is discussed in more detail in the Appendix).

and Sandstede & Scheel (2000), for instance: such perturbations are convected to $-\infty$, i.e. the pulses are convectively (transversely, to be more precise) unstable but are not absolutely unstable. Our results show that this is satisfied for $\delta > \delta^+ \approx 0.138$. Absolute and convective instabilities of the gKS pulses were also discussed by Chang *et al.* (1995).

For sufficiently small a, namely, $a < -\mathrm{Re}\,\lambda_2$, zero remains an eigenvalue of $\mathscr{L}_k^a$, which is now isolated and, therefore, belongs to the discrete spectrum. It can be easily seen that zero is an eigenvalue of $\mathscr{L}_k^a$ of both algebraic and geometric multiplicity unity with the corresponding eigenfunction $\boldsymbol{\Phi}_a^k = \mathrm{e}^{ax}\boldsymbol{\Phi}^k = \mathrm{e}^{ax}h_{kx}$. A simple computation shows that the adjoint operator $\mathscr{L}_k^{a*}$ is defined by $\mathscr{L}_k^{a*}f = \mathrm{e}^{-ax}\mathscr{L}_k^*(\mathrm{e}^{ax}f)$. Therefore, we conclude that for $a < -\mathrm{Re}\,\lambda_2$ zero is an eigenvalue of $\mathscr{L}_k^{a*}$ of both algebraic and geometric multiplicity unity with the corresponding eigenfunction $\boldsymbol{\Psi}_a^k = \mathrm{e}^{-ax}(\boldsymbol{\Psi}^k - \lim_{x\to-\infty}\boldsymbol{\Psi}^k)$. The projection onto the null space of $\mathscr{L}_k^a$ is given simply by $\Pi_k^a(f) = \langle f, \boldsymbol{\Psi}_a^k\rangle$. Applying projections Π_k^a to (2.10) rewritten in a weighted space leads to the same system (2.28) governing the locations of the pulses.

It should be noted that for a sufficiently large value of a, there may appear an eigenvalue of $\mathscr{L}_k^a$ which is not an eigenvalue of $\mathscr{L}_k$. Such an eigenvalue is called a "resonance pole" and is discussed in the Appendix.

Remark 1. Rigorous justifications of the derivations of systems similar to (2.28) have been done for the cases when zero is an eigenvalue of the operator $\mathscr{L}_k$ of equal algebraic and geometric multiplicities

and the primary pulse is spectrally stable, see Ei (2002) for the analysis for reaction–diffusion systems and a more recent work by Zelik & Mielke (2009) for the analysis of more general dissipative equations.

To be more precise, from Theorem 1.2 and also Corollary 10.3 and Remark 10.4 in Zelik & Mielke (2009), it follows that if the initial condition for an equation possessing a translational symmetry and a spectrally stable primary pulse with exponentially decaying tails is sufficiently close to a superposition of widely separated pulses, the corresponding solution remains close to a superposition of the pulses as long as the separation distances remain sufficiently large. Moreover, a system analogous to system (2.28) provides a leading-order description of the dynamics of the pulses with the error estimates for the right-hand sides being of order $O\big(\exp[-2(\min\{\lambda_1, -\mathrm{Re}\lambda_2\} - \varepsilon)l_*]\big)$ for some sufficiently small positive ε. It should be noted, that the use of exponential weights breaks the translational symmetry of the gKS equation, i.e. the equation for a function f obtained by substituting $h = \mathrm{e}^{-ax} f$ into the gKS equation does not possess translational symmetry but has a slightly different type of symmetry, see equation (4.1) below. To be more precise, if $f(x,t)$ is a solution of (4.1) then $\mathrm{e}^{ax_0} f(x-x_0,t)$ is also a solution (4.1) for any fixed x_0. Moreover, the nonlinearity in (4.1) is not just a function of f and its spatial derivatives (as is assumed in Zelik & Mielke, 2009) but is additionally multiplied by e^{-ax} **and therefore is not bounded in any reasonable non-weighted Sobolev space**. Thus, rigorous justification of the results for the gKS equation does not follow directly from Zelik & Mielke (2009) and is left as a topic for further investigation **– one could attempt to justify the reduction to the system governing the locations of the pulsed by first performing the analysis for the equation written in the weighted space and using periodic boundary conditions (in this case the exponential function appearing in the nonlinearity needs to be replaced by a suitable periodic approximation).** However, we note that an extensive numerical study presented in section 4. provides a strong evidence for the validity of the weak-interaction theory for the gKS equation.

We also note that some rigorous analytical results to explain the persistence of pulses and their interaction were obtained by Pego *et al.* (2007) who showed the stability of 1- and 2-solitons on an $O(\delta)$ time-scale for the case of large δ, which corresponds to the perturbed KdV equation, as was discussed in the introduction.

3. Bound-states theory

Since $l_k' = x_{k+1}' - x_k'$, the system governing the locations of the pulses can be transformed to the following one for the separation distances l_i's:

$$l_k' = S_2(l_k) + S_1(l_{k+1}) - S_2(l_{k-1}) - S_1(l_k), \tag{3.1}$$

for k such that both $k \in S$ and $k+1 \in S$. Note that if $k-1 \notin S$, then $S_2(l_{k-1})$ is replaced with zero and also if $k+2 \notin S$, then $S_1(l_{k+1})$ is replaced with zero. For a bound state of pulses, the distances l_k must be stationary. The case of a bound state of two pulses was discussed in Tseluiko *et al.* (2010). In this case

$$S_1(l_1) = S_2(l_1). \tag{3.2}$$

The functions S_1 and S_2 have the following behavior at infinity:

$$S_1(l) \sim D_1 \mathrm{e}^{-\lambda_1 l}, \tag{3.3}$$

$$S_2(l) \sim \mathrm{Re}(D_2 \mathrm{e}^{\lambda_2 l}), \tag{3.4}$$

where λ_1 and λ_2 are the roots of (2.6) that determine the left and the right tail of the pulse, respectively. Since λ_1 is always real, S_1 tends to zero in a monotonic manner. Also, λ_2 has a non-zero imaginary part

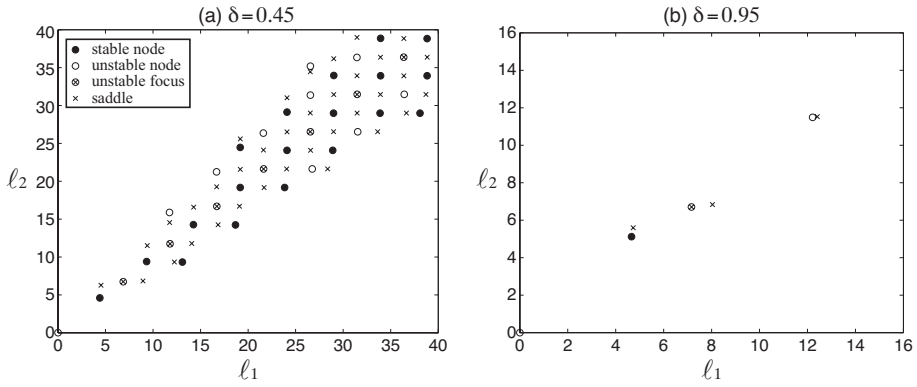

FIG. 6. Numerically computed bound states of three pulses for $\delta = 0.45$ and 0.95 (panels (a) and (b), respectively). The abscissas correspond to the distances between the first and the second pulse, and ordinates correspond to the distances between the second and the third pulse.

iff $\delta < \delta^* \approx 3.71$ meaning that S_2 tends to zero either in an oscillatory or monotonic manner depending on whether $\delta < \delta^*$ or $\delta \geqslant \delta^*$. Therefore, if $\mathrm{Im}\,\lambda_2 \neq 0$ and $\lambda_1 + \mathrm{Re}\,\lambda_2 > 0$, there is a countable infinite number of intersections of S_1 and S_2, i.e. there exists a countable infinite number of two-pulse bound states. Otherwise, there is a finite number of intersections of S_1 and S_2 (or no intersections at all), i.e. there exists a finite number of two-pulse bound states (or no bound states at all). The calculations for the gKS equation show that $\lambda_1 + \mathrm{Re}\,\lambda_2 < 0$ iff $\delta < \tilde{\delta} \approx 0.85$ (see Fig. 1(b)).

As noted in Tseluiko *et al.* (2010), this criterion for the existence of a countable infinite or finite number of two-pulse bound states coincides exactly with the Shilnikov-type criterion on the existence of an infinite countable or finite number of subsidiary homoclinic orbits, see Glendinning & Sparrow (1984). **Let us briefly recall Shilnikov's theory for our context (as is described in Glendinning & Sparrow, 1984). For a given δ, there exists a one-hump solitary pulse when $c = c_\delta$ and such a pulse can be considered as a homoclinic orbit to the origin in a three-dimensional phase space. (Note that for a one-hump solitary pulse c_δ is uniquely determined by δ.) Let us call this homoclinic orbit the primary homoclinic orbit. The origin is a saddle-focus if $\delta < \delta^* \approx 3.71$ with the linearised eigenvalues λ_1, λ_2 and $\bar{\lambda}_2$, where λ_1 is real and positive and λ_2 has a negative real part. The analysis then presented in section 3.2 of Glendinning & Sparrow (1984) implies that if $\lambda_1 + \mathrm{Re}\,\lambda_2 > 0$, there exists a countable infinite number of values of c, namely $c = c_1$, $c = c_2, \ldots$ (with the accumulation point c_δ), for which there exist subsidiary homoclinic orbits such that the unstable manifold of the origin passes once near the origin without homoclinicity being achieved and then arrives back into the origin. Such subsidiary homoclinic orbits correspond to two-pulse bound states. Note that the parameter c plays the role of the perturbation parameter in Shilnikov's theory.** It should be noted, however, that the weak-interaction approach not only can be used to analyse bound states but also provides the description of the leading-order dynamics of the pulses. Furthermore, it can be extended to higher dimensions and could be applied to, for example, non-local PDEs where the Shilnikov-type approach is not applicable.

In a similar way, bound states of any number of pulses can be analysed. For example, let us consider three-pulse bound states. The dynamics of the separation distances l_1 and l_2 for three pulses is described

by the following system:

$$l_1' = S_2(l_1) + S_1(l_2) - S_1(l_1), \tag{3.5}$$
$$l_2' = S_2(l_2) - S_2(l_1) - S_1(l_2). \tag{3.6}$$

Then, for a bound state of three pulses, we must have:

$$S_2(l_1) + S_1(l_2) - S_1(l_1) = 0, \tag{3.7}$$
$$S_2(l_2) - S_2(l_1) - S_1(l_2) = 0. \tag{3.8}$$

The numerically found solutions of (3.7) and (3.8), which correspond to three-pulse bound states are shown in the $l_1 l_2$-plane in Fig. 6 for $\delta = 0.45$ and 0.95 (panels (a) and (b), respectively). The abscissas show the distance l_1 between the first and the second pulse of a bound state, and the ordinates show the distance l_2 between the second and the third pulse. It can be observed that there is apparently a countable infinite number of three-pulse bound states for $\delta = 0.45$ and the bound-state separation distances l_1 and l_2 are concentrated around the line $l_1 = l_2$ in the $l_1 l_2$-plane. For $\delta = 1$, there are only two bound states. In fact, the following result is easily established: If $\lambda_1 + \mathrm{Re}\,\lambda_2 > 0$, there exists a countable infinite number of three-pulse bound states and the corresponding separation distances l_1 and l_2 satisfy $-(\mathrm{Re}\,\lambda_2/\lambda_1)l_1 - (1/\lambda_1)\log|D_2/D_1| < l_2 < -(\lambda_1/\mathrm{Re}\,\lambda_2)l_1 + (1/\mathrm{Re}\,\lambda_2)\log|D_1/D_2|$ for $l_1 \gg 1$ and $l_2 \gg 1$. Otherwise, if $\lambda_1 + \mathrm{Re}\,\lambda_2 < 0$, there exists a finite number of three-pulse bound states (or no bound states at all). As we can see in Fig. 6(b), for $\delta = 0.95$ there exist only six possible bound states. This criterion can be easily extended to any number of pulses.

4. Comparison of theory with computations

To validate the time-dependent pulse-interaction theory, we compared its predictions with numerical solutions of the full time-dependent equation (2.1). To solve (2.1) numerically, we implemented a pseudospectral method with a linear propagator so that the linear part of the spatial operator is resolved exactly in the Fourier space and the stiffness is removed (see, for example, Trefethen, 2000). As we discussed at the end of section 2., using exponential weights can make the pulses spectrally stable if $\delta > \delta^+ \approx 0.138$. This observation is useful, for example, for comparing the two-pulse evolution with the theory, as it suggests that using exponential weights could eliminate instabilities due to numerical noise and, therefore, allow us to track the pulse evolution for sufficiently long times. Hence, we substitute $h = \mathrm{e}^{-ax} f$ into (2.1) and obtain the following equation for f:

$$\begin{aligned} f_t - c_\delta f_x + a c_\delta f + (f_{xx} - 2a f_x + a^2 f) + \delta(f_{xxx} - 3a f_{xx} + 3a^2 f_x - a^3 f) \\ + (f_{xxxx} - 4a f_{xxx} + 6a^2 f_{xx} - 4a^3 f_x + a^4 f) + \mathrm{e}^{-ax}(f f_x - a f^2) = 0. \end{aligned} \tag{4.1}$$

Using hats to denote Fourier transforms and $\hat{u}(k,t) = \mathrm{e}^{-s(k)t}\hat{f}(k,t)$, where

$$s(k) = -(\mathrm{i}k - a)^4 - \delta(\mathrm{i}k - a)^3 - (\mathrm{i}k - a)^2 + c_\delta(\mathrm{i}k - a), \tag{4.2}$$

equation (4.1) can be transformed to the following form:

$$\hat{u}_t + \mathrm{e}^{-s(k)t}\mathscr{F}\left[\mathrm{e}^{-ax}\mathscr{F}^{-1}\left[\left(\frac{\mathrm{i}k}{2} - a\right)\mathscr{F}\left[(\mathscr{F}^{-1}[\mathrm{e}^{s(k)t}\hat{u}])^2\right]\right]\right] = 0, \tag{4.3}$$

where $\mathscr{F}$ and $\mathscr{F}^{-1}$ denote the Fourier and the inverse Fourier transforms, respectively. We use FFT to obtain the Fourier and the inverse Fourier transforms on periodic domains and propagate equation

(4.3) in time with the fourth-order Runge–Kutta method. **It should be emphasised that solving the gKS equation written in a weighted space and imposing sufficiently localised initial condition is equivalent to solving the equation in a non-weighted space (there is a one-to-one correspondence between these solutions given by $h = \mathrm{e}^{-ax} f$). Therefore, in principle solving numerically the equation in a non-weighted space and imposing periodic boundary conditions (and eliminating the numerical noise if one wishes to track the evolution for sufficiently long times) is equivalent to solving numerically the equation written in a weighted space and imposing sufficiently localised initial condition and periodic boundary conditions on sufficiently long spatial interval (as long as the solution remains sufficiently localised).**

In Figs. 7 and 8, we present the results of computational experiments for $\delta = 0.45$ and 0.95, respectively, where a superposition of two pulses was taken as an initial condition. In Figs. 9 and 10, we present the results of computational experiments for $\delta = 0.45$ and 0.95, respectively, where a superposition of three pulses was taken as an initial condition. In all the cases, the value of a for the exponential weight was chosen to be 0.2 ensuring that the primary pulses are spectrally stable in the exponentially weighted space. For Fig. 7(a), the initial pulse separation distance was taken to be 12. The dynamics in this case is repulsive. For Fig. 7(b), the initial pulse separation distance was taken to be 16, and the dynamics was found to be attractive. For both Figs. 7(a) and (b) the pulses tend to form a bound state with the separation distance of approximately 14.3. The solid lines in the figure were obtained by solving the model

$$l_1' = S_2(l_1) - S_1(l_1), \tag{4.4}$$

and we found very good agreement with the results obtained by solving (2.1) numerically in a weighted space with a superposition of two pulses as an initial condition (dashed lines).

For Fig. 8, the value of δ is 0.95. For Fig. 8(a), the initial pulse separation distance was taken to be 11. The dynamics in this case is attractive and the pulses form a bound state. However, if the initial separation distance is sufficiently large, the dynamics is only repulsive and the pulses do not form a bound state. This is demonstrated in Fig. 8(b), where the initial pulse separation distance was taken to be 12. We also observe that as the initial separation distance between the pulses is increased, the agreement between numerical and asymptotic results becomes better.

Figure 9 shows the evolution of the separation distances between three pulses for $\delta = 0.45$. For Fig. 9(a), the initial pulse separation distances were taken to be $l_1 = 11.89$ and $l_2 = 11.76$. (Recall that l_1 denotes the separation distance between the first and the second pulse and l_2 denotes the separation distance between the second and the third pulse.) For Fig. 9(a), we observe that the pulses tend to form a bound stated with nearly equal separation distances, approximately 9.5. The solid lines are obtained by solving the model in (3.5) and (3.6) numerically (the thin line shows the evolution of l_1 and the bold line shows the evolution of l_2). The dashed lines are obtained by solving the gKS equation numerically when the initial condition is a superposition of three pulses (the thin line shows the evolution of l_1 and the bold line shows the evolution of l_2). We observe that there is good agreement between the results obtained by solving the model in (3.5) and (3.6) and the results obtained by solving the gKS equation numerically, even though the separation distances are not so large. The agreement becomes better for larger separation distances between the pulses. This is demonstrated in Fig. 9(b), where the initial pulse separation distances were taken to be $l_1 = 16.8$ and $l_2 = 16.6$. In this case, the pulses apparently form a bound state with the separation between the first and the second pulse approximately 18.6 and the separation between the second and the third pulse approximately 14.3.

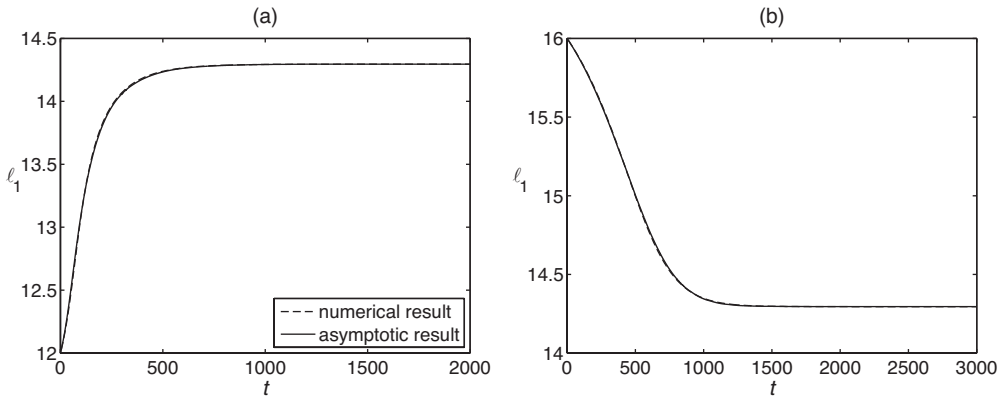

FIG. 7. Dependence of the pulse separation distance between two pulses on time for $\delta = 0.45$. Panels (a) and (b) show the evolution of the separation distances between two pulses when the initial separation distances are 12 and 16, respectively. Solid lines are obtained by solving numerically the model in (4.4). Dashed lines are obtained by solving numerically the gKS equation with a superposition of two pulses as an initial condition.

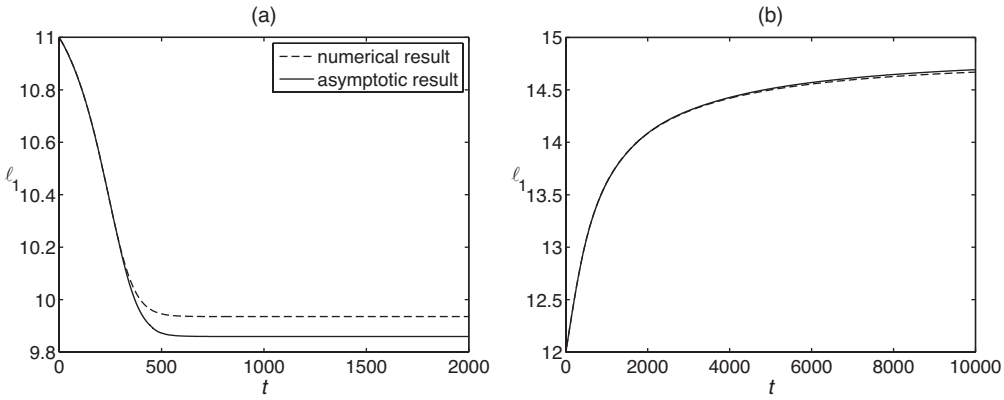

FIG. 8. Dependence of the pulse separation distance between two pulses on time for $\delta = 0.95$. Panels (a) and (b) show the evolution of the separation distances between two pulses when the initial separation distances are 11 and 12, respectively. Solid lines are obtained by solving numerically the model in (4.4). Dashed lines are obtained by solving numerically the gKS equation with a superposition of two pulses as an initial condition.

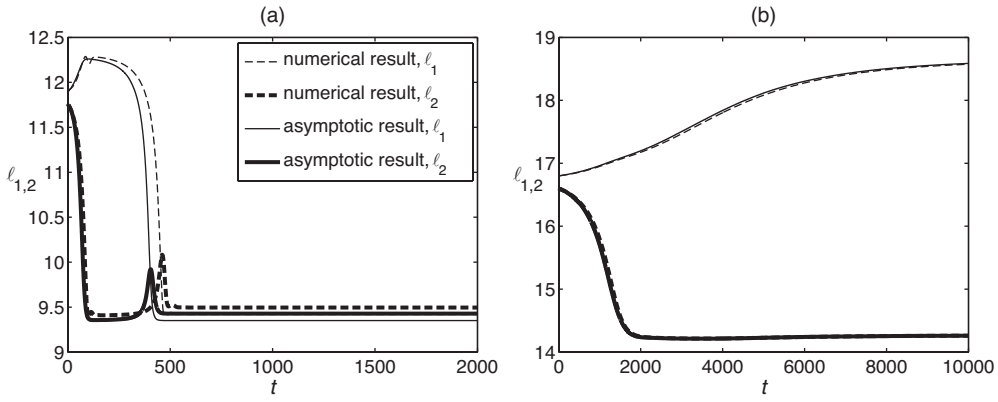

FIG. 9. Dependence of the pulse separation distances between three pulses on time for $\delta = 0.45$. Panels (a) and (b) show the evolution of the two-pulse separation distance when the initial separation distances are $l_1 = 11.89$, $l_2 = 11.76$ and $l_1 = 16.8$, $l_2 = 16.6$, respectively. Solid lines are obtained by solving numerically the model in (3.5) and (3.6). Dashed lines are obtained by solving numerically the gKS equation with a superposition of three pulses as an initial condition. The thin lines show the evolution of l_1. The bold lines show the evolution of l_2.

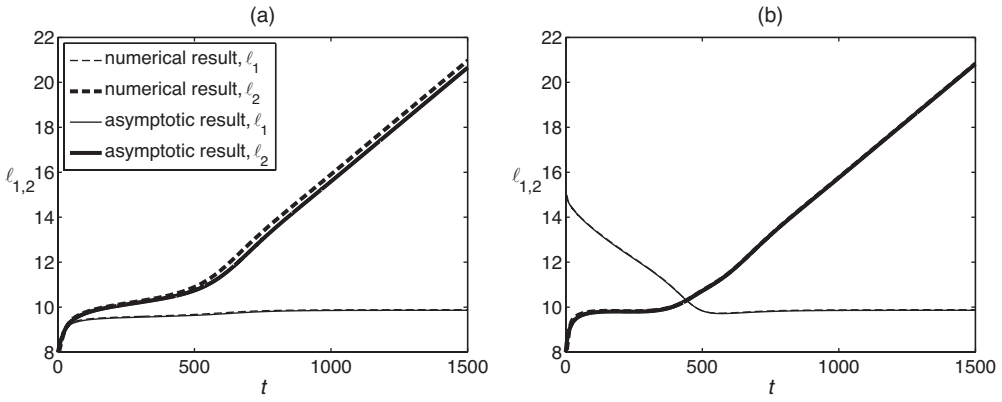

FIG. 10. Dependence of the pulse separation distances between three pulses on time for $\delta = 0.95$. Panels (a) and (b) show the evolution of the two-pulse separation distance when the initial separation distances are $l_1 = 8$, $l_2 = 8$ and $l_1 = 15$, $l_2 = 8$, respectively. Solid lines are obtained by solving numerically the model in (3.5) and (3.6). Dashed lines are obtained by solving numerically the gKS equation with a superposition of three pulses as an initial condition. The thin lines show the evolution of l_1. The bold lines show the evolution of l_2.

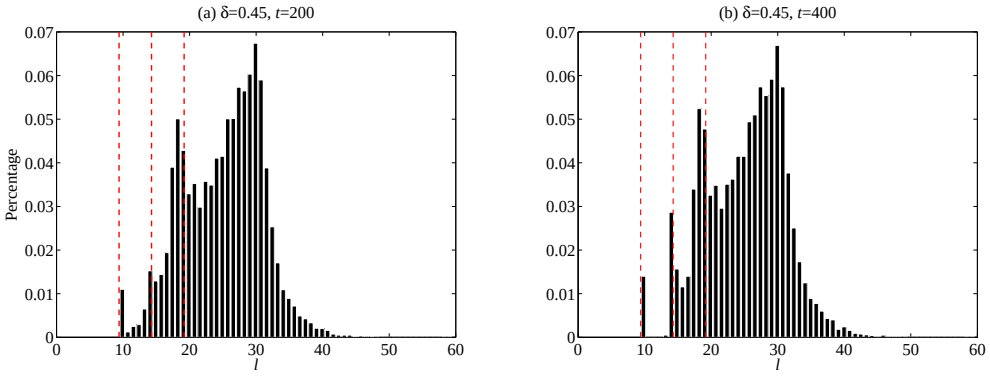

FIG. 11. (Colour online) Histogram for pulse separation distances based on a series of computational experiments for $\delta = 0.45$ at $t = 200$ and 400 (panels (a) and (b), respectively). **The red dashed line indicate pulse separation distances that correspond to the theoretically predicted stable two-pulse bound states.**

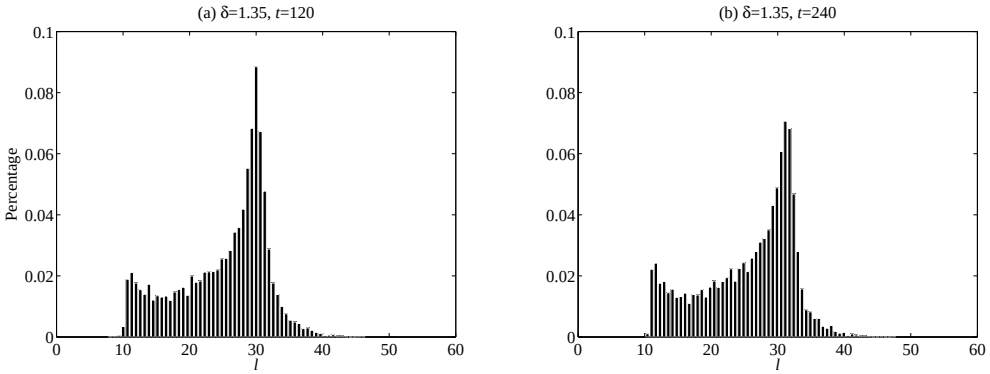

FIG. 12. Histogram for pulse separation distances based on a series of computational experiments for $\delta = 1.35$ at $t = 120$ and 240 (panels (a) and (b), respectively).

Figures 10(a) and (b) depict the evolution of the separation distances between three pulses for $\delta = 0.95$ when the initial separation distances are $l_1 = 8$, $l_2 = 8$ and $l_1 = 15$, $l_2 = 8$. In both cases, the first and the second pulse apparently form a bound state, which travels at a velocity smaller to that of the third pulse. Again, we observe that the agreement between the results obtained by solving the model in (3.5) and (3.6) and the results obtained by solving the gKS equation numerically are better for larger separation distances.

To further demonstrate the agreement between the theory and computations, we performed a series of numerical experiments for the gKS equation (2.1) in a non-weighted space ($a = 0$), where the initial condition was a localised ramdomly generated disturbance. The equation was solved on a periodic domain of half-length 1000 which was discretised into2^{13} intervals. The initial disturbance results in an expanding wave packet with pulses escaping the wave packet. We performed $1,500$ numerical experiments for each δ and computed the pulse separation distances data for each case. We took into account the first 8 pulses from each numerical experiment. In Fig. 11, we show the distributions of

separation distances for $\delta = 0.45$ at $t = 200$ and 400 (panels (a) and (b), respectively). This is done by plotting the histograms of the collected data that place the distances into 60 equally spaced intervals. As we can see, the distributions are characterised by the presence of peaks that become more pronounced in time. **The red dashed lines indicate pulse separation distances that correspond to the theoretically predicted stable two-pulse bound states. These occur at the distances l for which $S_1(l) = S_2(l)$. For this value of δ, there exist a countable infinite number of two-pulse bound states. However, just three of them are shown in the figure, namely** 9.4, 14.28 **and** 19.18**, and these are the separation distances around which the first three peaks in the histograms occur. The fact that in Fig. 11(b) the number values of l between the first two peaks is less than that in Fig. 11(a) indicates that the pulses tend to organise into bound states with well-defined separation distances, near the points where $S_1(l) = S_2(l)$). In fact, the same happens for the values of l between the second and the third peak – it can be observed that the number of values of l between these two peaks also decreases in time but on a slower timescale. Eventually, all the pulses will evolve into bound states and the histograms will be described only by sharp peaks.** In Fig. 12, we show the distribution of separation distances for $\delta = 1.35$ at $t = 120$ and 240 (panels (a) and (b), respectively). **In this case, the weak-interaction theory predicts one stable two-pulse bound state with the separation distance** 5.65 **and one unstable two-pulse bound state with the separation distance** 6.05**. However, the separation distance for the predicted stable two-pulse bound state is apparently not large enough for the weak-interaction theory to be valid, and, indeed, we can see that such a bound state does not appear in our numerical simulations.** We can see that the distributions are characterised by one main peak (which becomes less pronounced as t increases) and a thick left tail (which becomes thicker as t increases).

Remark 2. Finally, we would like to mention that Elphick *et al.* (1991) attempted to include the Galilean modes into the weak interaction theory and, in particular, for the case of two interacting pulses they derived the following second-order differential equation for the pulse separation distance, $l_1 = x_2 - x_1$:

$$l_1'' = S_2(l_1) - S_1(l_1) + l_1'[G_1(l_1) + G_2(l_1)], \tag{4.5}$$

where G_1 and G_2 are defined by

$$G_{1,2}(l) = -\int_{-\infty}^{\infty} h_*(x \mp l/2)\Psi_x(x \pm l/2)\,\mathrm{d}x. \tag{4.6}$$

Elphick *et al.*'s derivation appears to be not well justified. To be more precise, Elphick *et al.* (1991) claim that the projection onto the Galilean modes leads to the condition $\sum_{i=1}^{n} v_i' = 0$ (see their formula (31)), where $v_i = x_i'$, and their justification (see p. 1119) appears to be *ad hoc.* However, it can be easily shown (by projecting the dynamics onto the Gallilean modes) that the Gallilean modes are not excited in the evolution, and, therefore, the inclusion of these modes into the interaction theory does not change the resulting ordinary differential equations. (In fact, projecting the dynamics onto the Gallilean modes is equivalent to integrating over the whole spatial domain, and, therefore, the Galilean modes are not excited simply due to the conservation of mass.) In addition, we would like to mention that for the system of ordinary differential equations derived by Elphick *et al.* it is not clear how to extract initial conditions from a given initial condition $h(x, 0)$ that is close to a multi-pulse configuration. To be more precise, it is clear how initial locations of the pulses, $x_1(0), \ldots, x_n(0)$ can be determined (e.g. one can use conditions (2.23) shown above), but it is not clear how to determine the initial pulse velocities, $v_1(0), \ldots, v_n(0)$ for the given initial condition, $h(x, 0)$. In Fig. 13, we compare the results obtained by solving numerically the model

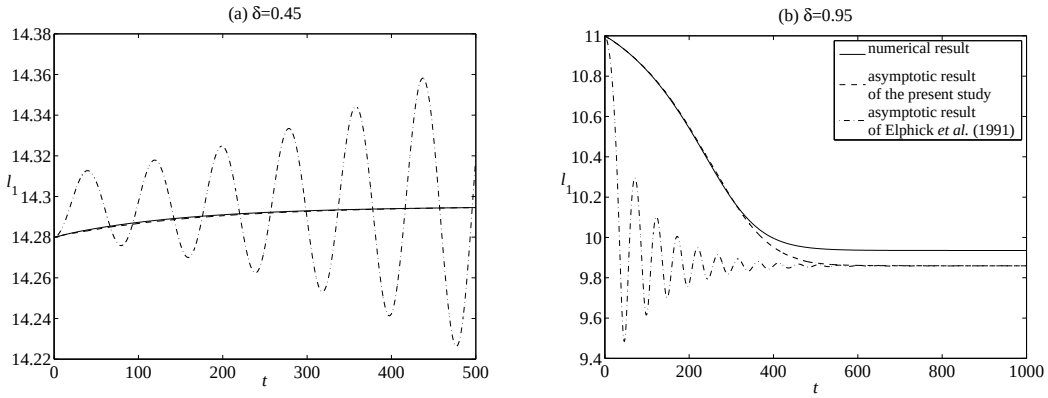

FIG. 13. **Dependence of the pulse separation distance between two pulses on time for (a) $\delta = 0.45$ and (b) $\delta = 0.95$. The initial separation distance is 14.28 and 11 for panels (a) and (b), respectively. The solid lines are obtained by solving numerically the gKS equation with a superposition of two pulses as an initial condition. The dashed lines are obtained by solving numerically the model in (4.4). The dash-dotted lines are obtained by solving numerically the model of Elphick *et al.* (1991), see equation (4.5).**

in (4.4) derived above and the results obtained by solving numerically the model of Elphick *et al.* (1991) (the dashed and dash-dotted lines, respectively) with the results obtained by solving numerically the gKS equation (the solid line) for $\delta = 0.45$ and $\delta = 0.95$ (panels (a) and (b), respectively) and for two pulsed with the initial separation distance $l_1 = 14.28$ and $l_1 = 11$ (panels (a) and (b), respectively). For the model of Elphick *et al.* (1991) we additionally choose, $l_1'(0) = 0$. It can be observed that the model in (4.4) produces results that are in much better agreement with the results obtained by solving the gKS equation numerically than the results produced by the model of Elphick *et al.* (1991). In panel (a), Elphick *et al.*'s model predicts oscillatory dynamics and the evolutions does not apparently converge to a bound state. In panel (b), although the evolution for Elphick *et al.*'s model apparently converges to the same bound state as the one predicted by the theory developed in the present study, it can be again observed that Elphick *et al.*'s model predicts oscillatory dynamics that is not found in the numerical simulation for the gKS equation.

5. Conclusions

We have developed a weak-interaction theory for the pulse solutions of the gKS equation, that is one of the simplest prototypes that describes nonlinear media with energy supply, dissipation, dispersion and nonlinearity. The underlying basis for the theory is that the spatio-temporal evolution of a solution to the gKS equation is dominated by localised nonlinear pulses which are stable and robust and continuously interact with each other (provided that the dispersion coefficient is sufficiently strong).

We represented the solution as a superposition of such pulses and an overlap function and we projected the dynamics of the overlap function onto translational modes that belong to the null spaces of the operators linearised around each pulse. To do these projections accurately, we carefully analysed the spectra of the linearised operators and the corresponding adjoint operators, and we have clarified certain ambiguities appearing in the literature on previous studies of the gKS equation. For instance, we

carefully analysed the null spaces of the operators, which are crucial for developing a pulse interaction theory based on appropriate projections onto the null spaces. We found that on an infinite domain zero is an eigenvalue of the linearised operators of geometric and algebraic multiplicity unity and is embedded into the essential spectrum. However, it is not an eigenvalue of the corresponding adjoint operators. The null spaces of the adjoint operators are spanned by a constant and a function having a jump at infinity. Despite this, we showed that projections onto the null spaces can be made rigorous in an appropriate exponentially weighted space, where the essential spectrum shifts to the left in the complex plane and zero becomes an isolated eigenvalue, and the derivation of a dynamical system describing interaction of the pulses due to translational modes can be accurately justified.

By analysing the fixed points of this system, we obtained bound states of any number of pulses. In particular, we analysed in detail bound states of two and three pulses. For two pulses, we showed the existence of a countable infinite or finite number of bound states, depending on the strength of the dispersive term in the equation. This criterion exactly coincides with Shilnikov's criterion on the existence of subsidiary homoclinic orbits. Our approach, however, in addition to providing an existence result for the bound states, also gives the description of the dynamics of the pulses. Besides, it can be extended to higher dimensions and could in principle be applied to non-local PDEs where the Shilnikov-type approach is not applicable. For three pulses, we showed that the bound states are concentrated around the diagonal in the $l_1 l_2$-plane, where l_1 and l_2 are the separation distances between the first and the second and the second and the third pulses, respectively. Our interaction theory and resulting bound states were corroborated by computational experiments for two and three pulses. In particular, we found that our theory predicts well pulse separation distances of true bound states while dynamic interaction of the pulses is well described by our simplified time-dependent model.

We have also performed a series of numerical experiments for the full gKS equation on a large periodic domain with a random initial condition and collected statistics on the separation distances of the pulses. The results showed that for the values of δ for which the theory predicts bound states, the histograms of the separation distances are characterised by pronounced peaks occurring at values corresponding to separation distances of the stable bound states obtained by the theory. The peaks become more pronounced in time. For larger values of δ the distributions of the pulse separation distances are rather unimodal with ticker left tails.

Acknowledgments

We thank Demetrios Papageorgiou and Marc Pradas for useful comments and suggestions. **We also thank the anonymous referees for several insightful comments that have helped us to improve the manuscript.** We acknowledge financial support by the Engineering and Physical Sciences Research Council of England through grant no. EP/F009194.

APPENDIX: RESONANCE POLE

For a sufficiently large value of a, there may appear an eigenvalue of $\mathscr{L}_k^a$ which is not an eigenvalue of $\mathscr{L}_k$. **We denote this negative eigenvalue by $-\lambda$ (so that $\lambda > 0$).** Such an eigenvalue is called a "resonance pole". The emergence of the resonance pole for $\delta = 0.5$ is shown in Figs. 5(b) and (c) for $a = 0.12$ and 0.42, respectively. In Fig. 5(c) we can see that as the essential spectrum is shifted sufficiently far to the left, one of the eigenvalues of the original operator $\mathscr{L}_k$ disappears. Let us denote by F_a and P_a the eigenfunction and the adjoint eigenfunction, respectively, that correspond to the resonance pole and

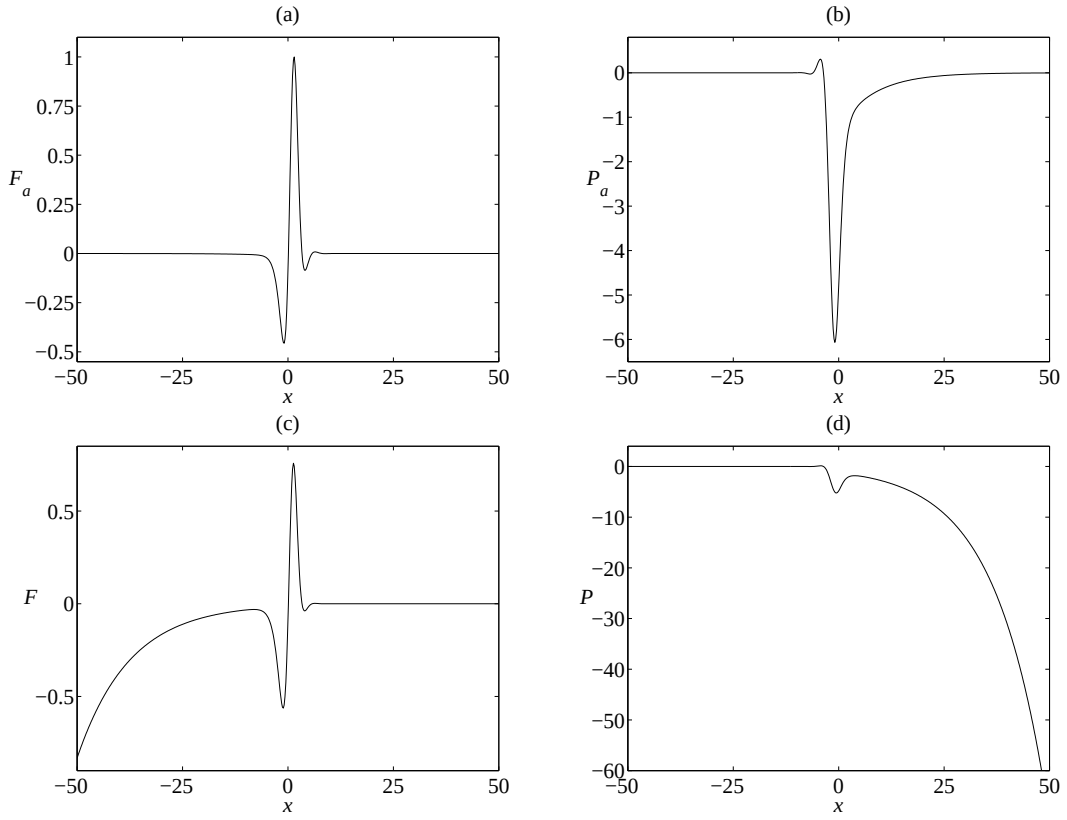

FIG. 14. **Eigenfunctions and adjoint eigenfunctions corresponding to the resonance pole when $\delta = 1.5$. Panels (a) and (b) show the eigenfunction F_a and the adjoint eigenfunction P_a in the exponentially weighted space with $a = 0.2$. Panels (c) and (d) show the eigenfunction F and the adjoint eigenfunction P in the the non-weighted space.**

by F and P, respectively, these functions in the non-weighted space, i.e. $F = \mathrm{e}^{-ax}F_a$ and $P = \mathrm{e}^{ax}P_a$. **The eigenfunction F_a and the adjoint eigenfunction P_a in the exponentially weighted space with $a = 0.2$ are shown in Figs. 14(a) and (b), respectively, for $\delta = 1.5$. The corresponding eigenfunction F and the adjoint eigenfunction P in the non-weighted space are shown in Figs. 14(c) and (d), respectively. It can be observed that the left tail of F and the right tail of P grow exponentially. Another observation is that the resonant eigenfunction F does not integrate to zero, i.e. the excitation of this mode should lead to the change of the mass of the excited pulse. Therefore, as was suggested by Chang *et al.* (1998), the resonance pole is responsible for the drainage mechanism of an exited pulse. We normalise the eigenfunctions so that**

$$\langle \Phi_a, \Psi_a \rangle = 1, \qquad \langle \Phi_a, P_a \rangle = 0, \tag{5.1}$$

$$\langle F_a, \Psi_a \rangle = 0, \qquad \langle F_a, P_a \rangle = 1. \tag{5.2}$$

where $\Phi_a = \mathrm{e}^{ax} h_{*x}$ and $\Psi_a = \mathrm{e}^{-ax}(\Psi - \lim_{x\to-\infty}\Psi)$. It can be seen that the above expressions are equivalent to the following ones:

$$\int_{-\infty}^{\infty} \Phi\,\Psi\,\mathrm{d}x = 1, \qquad \int_{-\infty}^{\infty} \Phi\,P\,\mathrm{d}x = 0, \tag{5.3}$$

$$\int_{-\infty}^{\infty} F\,\Psi\,\mathrm{d}x = 0, \qquad \int_{-\infty}^{\infty} F\,P\,\mathrm{d}x = 1, \tag{5.4}$$

(It should be noted that although the left tail of F and the right tail of P grow exponentially, the products appearing in all of the integrals above tend to zero exponentially as $|x| \to \infty$.) The eigenfunction and the adjoint eigenfunction for the operator $\mathscr{L}_k^a$ that correspond to the resonance pole are $F_a^k = \mathrm{e}^{ax_k} F_a(x - x_k)$ and $P_a^k = \mathrm{e}^{-ax_k} P_a(x - x_k)$, respectively, and in the non-weighted space $F^k = F(x - x_k)$ and $P^k = P(x - x_k)$, respectively.

Let us consider a single pulse located at $x_1(t)$, i.e. let

$$h(x,t) = h_*(x - x_1(t)) + \hat{h}(x,t), \tag{5.5}$$

where $\hat{h}(x,t)$ is assumed to be a small function decaying sufficiently fast at infinity which is free of the translational mode. The latter statement means that $x_1(t)$ is defined so that

$$\int_{-\infty}^{\infty} \big(h(x,t) - h_*(x - x_1(t))\big)\Psi(x - x_1(t))\,\mathrm{d}x = 0. \tag{5.6}$$

Projecting the dynamics onto the translational mode yields

$$\Big(1 - \int_{-\infty}^{\infty} \hat{h}\Psi_x^1\,\mathrm{d}x\Big)x_1' = \int_{-\infty}^{\infty} \hat{h}\hat{h}_x\Psi^1\,\mathrm{d}x, \tag{5.7}$$

where $\Psi^1(x,t) = \Psi(x - x_1(t))$. Next, considering the dynamics in an exponentially weighted space and projecting the dynamics onto the resonance pole, we find

$$\beta' = -\lambda\beta - x_1' \int_{-\infty}^{\infty} \hat{h}P_x^1\,\mathrm{d}x - \int_{-\infty}^{\infty} \hat{h}\hat{h}_x P^1\,\mathrm{d}x, \tag{5.8}$$

where $\beta(t) \equiv \int_{-\infty}^{\infty} \hat{h}P^1 1\,\mathrm{d}x$ is assumed to be small. **Let us now assume that**

$$\hat{h}(x,t) = \beta(t)F^1(x,t) + \tilde{h}(x,t), \tag{5.9}$$

where $\tilde{h}$ is free of both the translational mode and the resonant mode, i.e. in addition to (5.6), we require

$$\int_{-\infty}^{\infty} \big(h(x,t) - h_*(x - x_1(t)) - \beta(t)F(x - x_1(t))\big)P(x - x_1(t))\,\mathrm{d}x = 0, \tag{5.10}$$

which defines $\beta(t)$. (Note that in an exponentially weighted space the essential spectrum is located to the left of the resonance pole, and therefore its contribution to $\hat{h}$ decays very rapidly and $\hat{h}$ is mainly described by the resonant mode for large t) **Then, substituting (5.9) in (5.7) yields**

$$\Big(1 - \beta\int_{-\infty}^{\infty} F^1\Psi_x^1\,\mathrm{d}x - \int_{-\infty}^{\infty} \tilde{h}\Psi_x^1\,\mathrm{d}x\Big)x_1' = \beta^2\int_{-\infty}^{\infty} F^1F_x^1\Psi^1\,\mathrm{d}x + \beta\int_{-\infty}^{\infty} (F^1\tilde{h})_x\Psi^1\,\mathrm{d}x + \int_{-\infty}^{\infty} \tilde{h}\tilde{h}_x\Psi^1\,\mathrm{d}x. \tag{5.11}$$

Then, if we assume that $\tilde{h}$ is such that

$$\int_{-\infty}^{\infty} \tilde{h}\Psi_x^1 \,\mathrm{d}x = o(\beta), \qquad \int_{-\infty}^{\infty} (F^1\tilde{h})_x\Psi^1 \,\mathrm{d}x = o(\beta^2), \qquad \int_{-\infty}^{\infty} \tilde{h}\tilde{h}_x\Psi^1 \,\mathrm{d}x = o(\beta^3), \tag{5.12}$$

then $x_1' = O(\beta^2)$ and, neglecting $o(\beta^3)$ terms in (5.11), we find that the dynamics of the location of the pulse can be approximated by

$$x_1' = \frac{B\beta^2}{1-A\beta}, \tag{5.13}$$

where $A = \int_{-\infty}^{\infty} F_1\Psi_x^1 \,\mathrm{d}x$ and $B = \int_{-\infty}^{\infty} F_1F_{1x}\Psi^1 \,\mathrm{d}x = -\frac{1}{2}\int_{-\infty}^{\infty} F_1^2\Psi_x^1 \,\mathrm{d}x$. It was verified that B is positive. Therefore, adding a small disturbance to the pulse always leads to an increase of its speed, i.e. the pulse shifts downstream relative to its initial position. **Note that the analysis of Chang & Demekhin (2002) for large δ (see p. 230) implies that adding a small disturbance to the pulse may lead to the drift of the pulse both downstream and upstream, depending on the disturbance. However, our analysis (which is not restricted to the case of large δ) clearly shows that the analysis of Chang & Demekhin (2002) is not quite accurate – the pulse can drift only downstream. Then, substituting (5.9) in (5.8) yields**

$$\beta_t = -\lambda\beta - x_1'\beta\int_{-\infty}^{\infty} F^1P_x^1 \,\mathrm{d}x - x_1'\int_{-\infty}^{\infty} \tilde{h}P_x^1 \,\mathrm{d}x - \beta^2\int_{-\infty}^{\infty} F^1F_x^1P^1 \,\mathrm{d}x - \beta\int_{-\infty}^{\infty} (F^1\tilde{h})_xP^1 \,\mathrm{d}x - \int_{-\infty}^{\infty} \tilde{h}\tilde{h}_xP^1 \,\mathrm{d}x. \tag{5.14}$$

Assuming additionally that $\tilde{h}$ is such that

$$\int_{-\infty}^{\infty} \tilde{h}P_x^1 \,\mathrm{d}x = o(\beta), \qquad \int_{-\infty}^{\infty} (F^1\tilde{h})_xP^1 \,\mathrm{d}x = o(\beta^2), \qquad \int_{-\infty}^{\infty} \tilde{h}\tilde{h}_xP^1 \,\mathrm{d}x = o(\beta^3), \tag{5.15}$$

and neglecting $o(\beta^3)$ terms in (5.14), we obtain that the dynamics of the resonant mode can be approximated by

$$\beta' = -\lambda\beta - Cx_1'\beta - D\beta^2, \tag{5.16}$$

where $C = \int_{-\infty}^{\infty} F^1P_x^1 \,\mathrm{d}x$ and $D = \int_{-\infty}^{\infty} F^1F_x^1P^1 \,\mathrm{d}x$. The leading-order dynamics of the resonant mode is given by

$$\beta' = -\lambda\beta. \tag{5.17}$$

For the leading-order solution for the resonant mode, we obtain

$$\beta(t) = \beta(0)\mathrm{e}^{-\lambda t}. \tag{5.18}$$

Then,

$$x_1' = \frac{B\beta(0)^2\mathrm{e}^{-2\lambda t}}{1-A\beta(0)\mathrm{e}^{-\lambda t}}. \tag{5.19}$$

Integrating yields

$$x_1(t) = \frac{B}{\lambda A^2}\left[A\beta(0)\mathrm{e}^{-\lambda t} + \log(1-A\beta(0)\mathrm{e}^{-\lambda t}) - A\beta(0) - \log(1-A\beta(0))\right] + x_1(0). \tag{5.20}$$

Figure 15 shows the evolution of the pulse which is located initially at the origin and to which the following disturbance is initially added:

$$\hat{h}(x,0) = \alpha\,\mathrm{e}^{-x^2}. \tag{5.21}$$

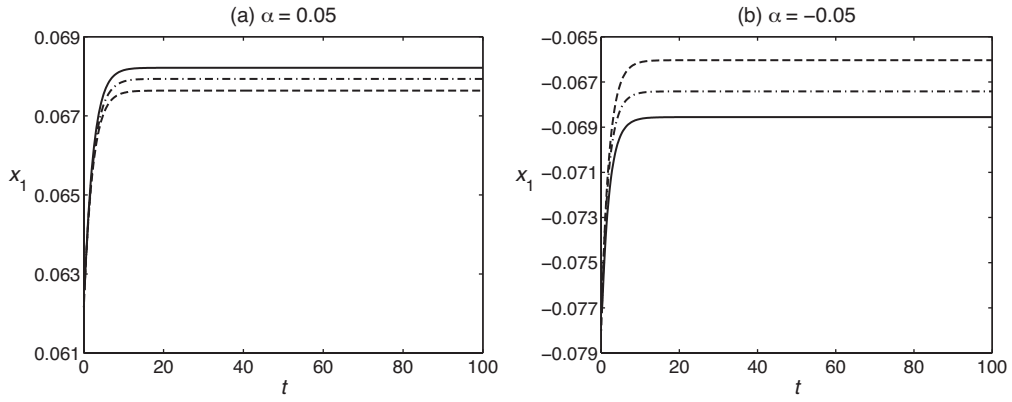

FIG. 15. Evolution of the pulse location **for the gKS equation with** $\delta = 1.5$ when the disturbance $\alpha\, e^{-x^2}$ is added initially. Panels (a) and (b) correspond to $\alpha = 0.05$ and $\alpha = -0.05$, respectively. The solid lines are obtained by solving the gKS equation numerically. The dot–dashed lines are obtained by solving the system of ordinary differential equations (5.8) and (5.13) numerically. The dashed lines show the function (5.20).

The value of δ is 1.5. In panel (a), $\alpha = 0.05$. In panel (b), $\alpha = -0.05$. The solid lines show the evolution of the pulse obtained by solving the gKS equation numerically (the numerical scheme used to solve the gKS equation numerically is discussed in detail in section 4.). The dashed lines are obtained by solving the system of ordinary differential equations (5.13) and (5.16) numerically. The dot–dashed lines show the functions (5.20). It should be noted that the disturbance (5.21) is not free of the translational mode if the pulse is located at the origin. That is why $x_1(0) \approx 0.062$ and $x_1(0) \approx -0.078$ for $\alpha = 0.05$ and $\alpha = -0.05$, respectively. As we can see, there is good agreement between the numerical solution of the gKS equation and the asymptotic results (it was verified that the agreement becomes better for smaller values of $|\alpha|$). We can also note that the numerical solution of equations (5.13) and (5.16) provides a slightly better approximation than the function (5.20).

Our preliminary consideration shows that the resonance pole may be important for the interaction of pulses – projecting the dynamics not only onto the translational modes but also on the resonant modes should lead to a coupled system of ordinary differential equations for the evolution of the locations of the pulses and the coefficients of the resonant modes. This should describe weak interaction of the pulses more precisely. An accurate derivation and analysis of such a system is left as a topic for future research.

References

CHAMPNEYS, A.R. & SANDSTEDE, B. (2007) Numerical computation of coherent structures, In: B. KRAUSKOPF, H.M. OSINGA AND J. GALAN-VIOQUE, eds. *Numerical Continuation Methods for Dynamical Systems.* Springer, 331–358.

CHANG, H.-C. & DEMEKHIN, E.A. (2002) *Complex wave dynamics on thin films*, Elsevier Scientific.

CHANG, H.-C., DEMEKHIN, E.A. & KALAIDIN, E. (1998) Generation and suppression of radiation by solitary pulses, *SIAM J. Appl. Math.*, **58**, 1246–1277.

CHANG, H.-C., DEMEKHIN, E.A. & KOPELEVICH, D.I. (1995) Stability of a solitary pulse against wave packet disturbances in an active medium, *Phys. Rev. Lett.*, **75**, 1747–1750.

COHEN, B.I., KROMMES, J.A., TANG, W.M. & ROSENBLUTH, M.N. (1976) Non-linear saturation of the dissipative trapped ion mode by mode coupling, *Nucl. Fusion*, **16**, 971–992.

DAVIES, E.B. (2002) Non-self-adjoint differential operators, *Bulletin of the London Mathematical Society*, **34**, 513–532.

DUPRAT, C., GIORGIUTTI-DAUPHINÉ, F., TSELUIKO, D., SAPRYKIN, S. & KALLIADASIS, S. (2009) Liquid film coating a fiber as a model system for the formation of bound states in active dispersive–dissipative nonlinear media, *Phys. Rev. Lett.*, **103**, 234501.

EDMUNDS, D.E. & EVANS, W.D. (1987) *Spectral theory and differential operators*, Clarendon Press.

EI, S.-I. (2002) The motion of weakly interacting pulses in reaction–diffusion systems, *J. Dyn. Differ. Equ.*, **14**, 85–137.

EI, S.-I. & OHTA, T. (1994) Equation of motion for interacting pulses, *Phys. Rev. E*, **50**, 4672–4678.

ELPHICK, C., IERLEY, G.R., REGEV, O. & SPIEGEL, E.A. (1991) Interacting localized structures with Galilean invariance, *Phys. Rev. A*, **44**, 1110–1122.

FRISCH, U., SHE, Z.S. & THUAL, O. (1986) Viscoelastic behavior of cellular solutions to the Kuramoto–Sivashinsky model, *J. Fluid Mech.*, **168**, 221–240.

GLENDINNING, P. & SPARROW, C. (1984) Local and global behaviour near homoclinic orbits, *J. Stat. Phys.*, **35**, 645–96.

HOMSY, G.M. (1974) Model equations for wavy viscous film flow, *In: Lectures in Applied Mathematics: Nonlinear Wave Motion*, **15**, 191–194.

HYMAN, J.M., NICOLAENKO, B. & ZALESKI, S. (1986) Order and complexity in the Kuramoto–Sivashinsky model of weakly turbulent interfaces, *Physica D*, **23**, 265–292.

JURMAN, L.A. & MCCREADY, M.J. (1989) Study of waves on thin liquid films sheared by turbulent gas flows, *Phys. Fluids A*, **1**, 522–536.

KALLIADASIS, S., DEMEKHIN, E.A., RUYER-QUIL, C. & VELARDE, M.G. (2003) Thermocapillary instability and wave formation on a film flowing down a uniformly heated plane, *J. Fluid Mech.*, **492**, 303–338.

KALLIADASIS, S., RUYER-QUIL, C., SCHEID, B. & VELARDE, M.G. (2012) *Falling Liquid Films*, Springer Series on Applied Mathematical Sciences, London.

KAWAHARA, T. (1983) Formation of saturated solitons in a nonlinear dispersive system with instability and dissipation, *Phys. Rev Lett.*, **51**, 381–383.

KAWAHARA, T. & TOH, S. (1988) Pulse interaction in an unstable dissipative-dispersive nonlinear system, *Phys. Fluids*, **11**, 2103–2111.

KURAMOTO, Y. (1978) Diffusion-induced chaos in reaction systems, *Prog. Theor. Phys. Suppl.*, **64**, 346–367.

LIN, S.P. (1974) Finite amplitude side-band stability of a viscous film, *J. Fluid Mech.*, **63**, 417–429.

P. MANNEVILLE (1990) *Dissipative Structures and Weak Turbulence*, Academic Press, New York.

NEPOMNYASHCHY, A.A. (1974) Stability of wave regimes in a film flowing down on inclined plane, *Fluid Dyn.*, **9**, 354–359.

ORON, A. & EDWARDS, D.A. (1993) Stability of a falling liquid film in the presence of interfacial viscous stress, *Phys. Fluids A*, **5**, 506–508.

PEGO, R.L. & WEINSTEIN, M.I. (1992) Eigenvalues, and instabilities of solitary waves, *Phil. Trans. R. Soc. Lond. A*, **340**, 47–94.

PEGO, R.L. & WEINSTEIN, M.I. (1994) Asymptotic stability of solitary waves, *Commun. Math. Phys.*, **164**, 305–349.

PEGO, R.L., SCHNEIDER, G.S. & UECKER, H. (2007) Long-time persistence of Korteweg–de Vries solitons as transient dynamics in a model of inclined film flow, *P. Roy. Soc Edinb. A*, **137**, 133–146.

SANDSTEDE, B. & SCHEEL, A. (2000) Absolute and convective instabilities of waves on unbounded and large bounded domains, *Physica D*, **145**, 233–277.

SANDSTEDE, B. (2002) Stability of travelling waves, In: B. FIEDLER, ed. *Handbook of Dynamical Systems II*, North-Holland, 983–1055.

SAPRYKIN, S., DEMEKHIN, E.A. & KALLIADSIS, S. (2005) Two-dimensional wave dynamics in thin films. I. Stationary solitary pulses, *Phys. Fluids*, **17**, 117105.

SIVASHINSKY, G.I. (1977) Nonlinear analysis of hydrodynamic instability in laminar flames. Part 1, *Acta Astronaut.*, **4**, 1176–1206.

TREFETHEN, L.N. (2000) *Spectral methods in Matlab*, Society for Industrial and Applied Mathematics, Philadelphia, PA.

TREVELYAN, P.M.J. & KALLIADASIS, S. (2004) Dynamics of a reactive falling film at large Péclet numbers. I. Long-wave approximation, *Phys. Fluids*, **16**, 3191–3208.

TSELUIKO, D., SAPRYKIN, S., DUPRAT, C., GIORGIUTTI-DAUPHINÉ, F. & KALLIADASIS, S. (2010) Pulse dynamics in low-Reynolds-number interfacial hydrodynamics: Experiments and theory, *Physica D*, 239, 2000–2010.

ZELIK, S. & MIELKE, A. (2009) Multi-pulse evolution and space-time chaos in dissipative systems, *Memoirs Amer. Math. Soc.*, **198**, 1–95.